



THE UNIVERSITY *of* EDINBURGH

Edinburgh Research Explorer

Modelling the Influence of RKIP on the ERK Signalling Pathway Using the Stochastic Process Algebra PEPA

Citation for published version:

Calder, M, Gilmore, S & Hillston, J 2006, Modelling the Influence of RKIP on the ERK Signalling Pathway Using the Stochastic Process Algebra PEPA. in C Priami, A Ingolfsson, B Mishra & H Riis Nielson (eds), *Transactions on Computational Systems Biology VII*. Lecture Notes in Computer Science, vol. 4230, Springer-Verlag GmbH, pp. 1-23. https://doi.org/10.1007/11905455_1

Digital Object Identifier (DOI):

[10.1007/11905455_1](https://doi.org/10.1007/11905455_1)

Link:

[Link to publication record in Edinburgh Research Explorer](#)

Document Version:

Peer reviewed version

Published In:

Transactions on Computational Systems Biology VII

General rights

Copyright for the publications made accessible via the Edinburgh Research Explorer is retained by the author(s) and / or other copyright owners and it is a condition of accessing these publications that users recognise and abide by the legal requirements associated with these rights.

Take down policy

The University of Edinburgh has made every reasonable effort to ensure that Edinburgh Research Explorer content complies with UK legislation. If you believe that the public display of this file breaches copyright please contact openaccess@ed.ac.uk providing details, and we will remove access to the work immediately and investigate your claim.



Modelling the influence of RKIP on the ERK signalling pathway using the stochastic process algebra PEPA

Muffy Calder¹, Stephen Gilmore² and Jane Hillston²

¹ Department of Computing Science, The University of Glasgow, Glasgow, Scotland.
email muffy@dcs.gla.ac.uk

² Laboratory for Foundations of Computer Science, The University of Edinburgh,
Scotland. email stg@inf.ed.ac.uk, jeh@inf.ed.ac.uk

Abstract. This paper examines the influence of the Raf Kinase Inhibitor Protein (RKIP) on the Extracellular signal Regulated Kinase (ERK) signalling pathway [5] through modelling in a Markovian process algebra, PEPA [11]. Two models of the system are presented, a reagent-centric view and a pathway-centric view. The models capture functionality at the level of subpathway, rather than at a molecular level. Each model affords a different perspective of the pathway and analysis. We demonstrate the two models to be formally equivalent using the timing-aware bisimulation defined over PEPA models and discuss the biological significance.

1 Introduction

In recent years several authors have investigated the use of Petri nets and process algebras – techniques originating in theoretical computer science – for representing the biochemical pathways within and between cells [15, 18, 10]. Largely, the previous work has focussed on capturing the appropriate functionality at the molecular level and analysis is through simulation. In this paper we present a preliminary exploration of an alternative approach in which a more abstract approach is taken and the target mathematical representation is a continuous time Markov chain. This involves the analytical application of a process algebra to a biochemical pathway with feedback. Our goal is to develop more than one representation, suitable for different forms of analysis. We prove the two representations to be equivalent (i.e. bisimilar).

The process algebra which we use is Hillston’s PEPA [11], a Markovian process algebra which incorporates stochastic durations and probabilistic choices. The system which we consider is the Ras/Raf-1/MEK/ERK signalling pathway, as presented in [5]. We believe that our modelling is novel because we are able to combine performance and different modelling viewpoints. Moreover we demonstrate the feasibility of using process algebra to model signalling pathways in a more abstract style than previously.

We propose that process algebra models are appropriate in this domain for several reasons. First, an algebraic formulation of the model makes clear the

interactions between the biochemical entities, or substrates. This is not always apparent in the classical, ordinary differential equation (ODE) models. Second, an algebraic approach permits comparison of high level descriptions. For example, when one is first building up a picture of a pathway from experimental evidence, it may be natural to describe the pathway in a fine-grained, distributed fashion, e.g. each substrate (in this case a protein) is described in terms of its interactions. That is, each (collection of a) protein is a process and all processes run in parallel, synchronising accordingly. But later, we may prefer a higher level view of a pathway which describes how a pathway is composed of (perhaps already well known) sub-pathways. Indeed we may wish to derive the latter from the former, or vice-versa. Third, a stochastic process approach allows reasoning about livelocks, deadlocks, and the performance of the behaviour of the pathway in the long-run.

This paper is an extended version of the earlier paper [2]. As previously, we concentrate primarily on alternative approaches to constructing a representation of a pathway. We show that two contrasting representations can indeed be identified. Moreover they can be formally shown to be equivalent. The novelty of this paper lies in the systematic transformation between the alternative representations which are presented in algorithmic form. The analysis of the model has also been somewhat extended.

In the next section we give a brief overview of cell signalling and the Ras/Raf-1/MEK/ERK pathway. In section 3 we give two different PEPA formulations of the pathway: the first is reagent-based (i.e. distributed) and the second is pathway-based. In section 4 we compare the two models and show them to be bisimilar. Section 5 contains some analysis of the underlying continuous time Markov model. Transformation between the two styles of representation is presented in section 6. There follows a discussion of further analysis, related work and our conclusions.

2 RKIP and the ERK Pathway

The most fundamental cellular processes are controlled by extracellular signalling [7]. This signalling, or communication between cells, is based upon the release of signalling molecules, which migrate to other cells and deliver stimuli to them (e.g. protein phosphorylation). Cell signalling is of special interest to cancer researchers because when cell signalling pathways operate abnormally, cells divide uncontrollably.

The Ras/Raf-1/MEK/ERK pathway (also called Ras/Raf, or ERK pathway) is a ubiquitous pathway that conveys mitogenic and differentiation signals from the cell membrane to the nucleus. Briefly, Ras is activated by an external stimulus, it then binds to and activates Raf-1 (to become Raf-1*, “activated” Raf) which in turn activates MEK and then ERK. This “cascade” of protein interaction controls cell differentiation, the effect being dependent upon the activity of ERK. A current area of experimental scientific investigation is the role the kinase inhibitor protein RKIP plays in the behaviour of this pathway: the hy-

pothesis is that it inhibits activation of Raf and thus can “dampen down” the ERK pathway. Certainly there is much evidence that RKIP inhibits the malignant transformation by Ras and Raf oncogenes in cell cultures and it is reduced in tumours. Thus good models of these pathways are required to understand the role of RKIP and develop new therapies. Moreover, an understanding of the functioning and structure of this pathway may lead to more general results applicable to other pathways.

Here, we consider how RKIP regulates the activity of the Raf-1/MEK/ERK module of the ERK pathway, as presented in [5]. This paper [5] presents a number of mathematical models in the form of nonlinear ODEs and difference equations representing the (enzyme) kinetic reactions, based on a graphical representation given in Figure 1. This figure is taken from [5], with some additions. Specifically, we have added MEK and an associated complex, following discussions with the authors¹.

We take Figure 1 as our starting point, and explain informally, its meaning. Each node is labelled by the protein (or substrate, we use the two interchangeably) it denotes. For example, Raf-1, RKIP and Raf-1*/RKIP are proteins, the last being a complex built up from the first two. It is important to note that Raf-1*/RKIP is simply a *name*, following biochemical convention; the / symbol is not an operator (in this context). A suffix -P or -PP denotes a phosphorylated protein, for example MEK-PP and ERK-PP. Each protein has an associated concentration, denoted by m_1 , m_2 etc. *Reactions* define how proteins are built up and broken down. We refer to the former as an association, or forward reaction, and the latter as a disassociation, or backward reaction. Associations are typically many to one, and disassociations one to many, relations. In the figure, bi-directional arrows denote both forward and backward reactions; uni-directional arrows denote disassociations. For example, Raf-1* and RKIP react (forwards) to form Raf-1*/RKIP, and Raf-1/RKIP disassociates (a backward reaction) into Raf-1* and RKIP. Reactions do not necessarily come in pairs; for example, Raf-1*/RKIP/ERK-PP disassociates into Raf-1*, ERK and RKIP-P. Each reaction has a rate denoted by the rate constants k_1 , k_2 , etc. These are given in the rectangles, with $kn/kn + 1$ denoting that kn is the forward rate and $kn + 1$ the backward rate. So for example, Raf-1* and RKIP react (forwards) with rate k_1 , and Raf-1/RKIP disassociates with rate k_2 .

Initially, all concentrations are unobservable, except for m_1 , m_2 , m_7 , m_9 , and m_{10} [5].

Figure 1 gives only a static, abstract view of the pathway; the dynamic behaviour is quite complex, particularly because some substrates are involved in more than one reaction. In the next section we develop two process algebraic models which capture that dynamic behaviour.

¹ Analysis of our original model(s) indicated a problem with MEK and prompted us to contact an author of [5] who confirmed that there was an omission.

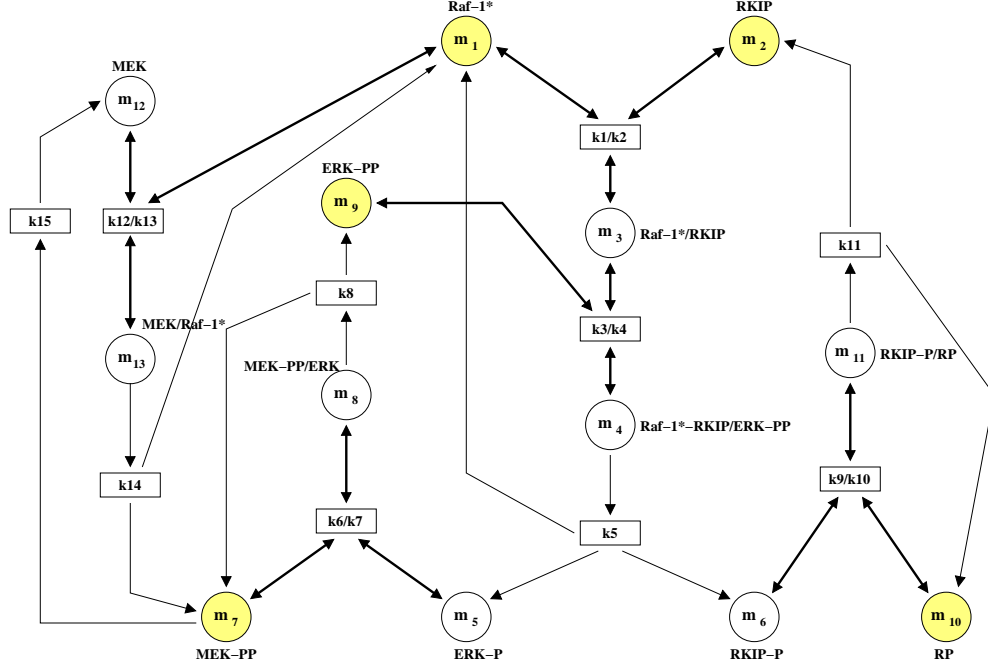


Fig. 1. RKIP inhibited ERK pathway

3 Modelling the ERK signalling pathway in PEPA

In this section we present two stochastic process algebra models of the ERK signalling pathway.

The two models presented here encode different views of the underlying biochemistry. The first is a reagent-centric view, focussing on the variations in concentrations of the reagents, fluctuating with phosphorylation and product formation, i.e. with association and disassociation reactions. This model provides a fine-grained, distributed view of the system. The second is a pathway-centric view, tracking the legitimate serialisations of activities. This model provides a coarser grained, more abstract view of the same system.

For some purposes in biological study the former view provides the right conceptual tools and powers the programme of analysis. For other purposes the pathway-centric view brings to the fore the dynamics of greatest interest. A major contribution of this paper is the unification of both views.

We express both models in the PEPA stochastic process algebra [11]. We assume some familiarity with this process algebra; a brief introduction to PEPA is contained in Appendix A. All activities in PEPA are timed. Specifically, their durations are quantified using exponentially-distributed random variables. The PEPA algebra supports multi-way cooperations between components: the result of synchronising on an activity α is thus another α , available for further syn-

chronisation. The multi-way synchronisation of PEPA makes this process algebra ideally suited to this domain.

Each reaction in the pathway is represented by a multi-way synchronisation – on the reagents of the reaction². We refer to reagents as *producers* and *consumers*, depending upon their role within the reaction. Table 1 gives the producers and consumers for reactions in the pathway. The first column names the reaction using the following convention. Reactions which are forward and backward are called *react*, with a prefix which is the associated rate constant. For example, *k1react* is the name of the reaction between Raf-1* and RKIP, to produce Raf-1*/RKIP. Thus *k1react* is a 3-way synchronisation. Reactions which are only disassociations are called *product* (because they produce *products*); again, the prefix denotes the associated rate constant. Table 1 gives only the forward reactions for the reactions which are both forward and backwards; to obtain the associated backward descriptions, replace Producer by Consumer and vice-versa.

Reaction	Producer(s)	Consumer(s)
<i>k1react</i>	{ Raf-1*, RKIP }	{ Raf-1*/RKIP }
<i>k3react</i>	{ ERK-PP, Raf-1*/RKIP }	{ Raf-1*/RKIP/ERK-PP }
<i>k6react</i>	{ MEK-PP, ERK-P }	{ MEK-PP/ERK }
<i>k9react</i>	{ RKIP-P, RP }	{ RKIP-P/RP }
<i>k12react</i>	{ MEK, Raf-1* }	{ MEK/Raf-1* }
<i>k5product</i>	{ Raf-1*/RKIP/ERK-PP }	{ ERK-P, RKIP-P, Raf-1* }
<i>k8product</i>	{ MEK-PP/ERK }	{ MEK-PP, ERK-PP }
<i>k11product</i>	{ RKIP-P/RP }	{ RKIP, RP }
<i>k14product</i>	{ MEK/Raf-1* }	{ Raf-1*, MEK-PP }
<i>k15product</i>	{ MEK-PP }	{ MEK }

Table 1. Reactions in the pathway

3.1 Modelling centred on reagents

The reagent-centred model is presented in Figures 2 and 3. In this view, we represent concentrations by a discrete number of abstract values. Here, we consider the coarsest possible discretisation: there are two values representing (continuous) concentrations; we refer to the two values as *high* and *low*. The former implies that a reagent *can* participate (as a producer) in a forward reaction; the latter implies that a reagent *can* participate (as a consumer) in a product, or (as a producer) in a backward reaction. Otherwise, the substrate is inert, with respect to a reaction. We discuss the effect of a finer granularity of abstract concentration on the model in Section 7.

² We agree with the authors of [15] – reactions are fundamentally synchronous.

We define the behaviour of each substrate in turn, for each concentration. Thus there are $2n$ equations, where n is the number of proteins. We adopt the naming convention that high concentrations have a H subscript and low concentrations have a L subscript.

Most equations involve a choice between alternative behaviours (notated by $+$). For example, even in one of the simplest cases, RKIP, where there is a simple cycle between high and low concentrations, there is still a choice of how to return to a high concentration (by a backwards reaction, or through a product). Most behaviours are more complex.

The equations define the possible reactions within the pathway. All of the permissible interleavings of these reactions are obtained from the (synchronised) parallel composition of these components. Figure 3 shows how these are composed in the PEPA algebra. The composition operator (\bowtie) is indexed by an activity set (i.e. the events whose participants must be synchronised). The left and right operands must cooperate on these activities, introducing a synchronisation point. The degenerate case of this composition operator (where the set is empty) provides the expected unrestricted parallel composition of the components, allowing all possible interleavings without synchronisation. This case is denoted by \parallel (there is one occurrence).

The initial state of the model has high concentrations of some reagents and low concentrations of the others, as described in the previous section. Therefore, in Figure 3, proteins with an initial concentration are initially high; all others are low.

3.2 Modelling centred on pathways

A different view is afforded by the pathway-centric perspective. This de-emphasises reagents and emphasises sub-pathways within the signalling pathway. In this model, given in Figure 4, there are five (sub)pathways, one for each substrate with an initial concentration. Thus *Pathway*₁₀ corresponds to the pathway from RP (m_{10}), *Pathway*₂₀ to RKIP (m_2), *Pathway*₃₀ to ERK-PP (m_9), *Pathway*₄₀ to Raf-1* (m_1), and *Pathway*₅₀ to MEK-PP (m_7). Each (sub)pathway describes, in effect, how a substrate is consumed and then, eventually, replenished.

It is important to note that none of these (sub)pathways is *closed*, i.e. there are reactions with edges which are directed to/from outside of the (sub)pathway. Figure 6 gives a diagrammatic representation of the simplest pathway, *Pathway*₁₀. In this case, the pathway is not closed because there are two missing edges associated with *k9react* and *k11product*.

This presentation facilitates the direct verification of simple properties of the model such as “the first observable activity is event X ”. For example, an initial syntactic inspection of this model would lead to the conclusion that the first activity is one of *k1react*, *k3react*, *k9react* or *k15product*. Processing the model with the PEPA Workbench [9] confirms that the initial model configuration allows only *k15product* and *k1react*, the others are not permitted because some necessary participants are not initially ready to engage in these reactions.

$$\begin{aligned}
\text{Raf-1}_H^* &\stackrel{\text{def}}{=} (k1react, k_1). \text{Raf-1}_L^* + (k12react, k_{12}). \text{Raf-1}_L^* \\
\text{Raf-1}_L^* &\stackrel{\text{def}}{=} (k5product, k_5). \text{Raf-1}_H^* + (k2react, k_2). \text{Raf-1}_H^* \\
&\quad + (k13react, k_{13}). \text{Raf-1}_H^* + (k14product, k_{14}). \text{Raf-1}_H^* \\
\text{RKIP}_H &\stackrel{\text{def}}{=} (k1react, k_1). \text{RKIP}_L \\
\text{RKIP}_L &\stackrel{\text{def}}{=} (k11product, k_{11}). \text{RKIP}_H + (k2react, k_2). \text{RKIP}_H \\
\text{MEK}_H &\stackrel{\text{def}}{=} (k12react, k_{12}). \text{MEK}_L \\
\text{MEK}_L &\stackrel{\text{def}}{=} (k13react, k_{13}). \text{MEK}_H + (k15product, k_{15}). \text{MEK}_H \\
\text{MEK/Raf-1}_H^* &\stackrel{\text{def}}{=} (k14product, k_{14}). \text{MEK/Raf-1}_L^* + (k13react, k_{13}). \text{MEK/Raf-1}_L^* \\
\text{MEK/Raf-1}_L^* &\stackrel{\text{def}}{=} (k12react, k_{12}). \text{MEK/Raf-1}_H^* \\
\text{MEK-PP}_H &\stackrel{\text{def}}{=} (k6react, k_6). \text{MEK-PP}_L + (k15product, k_{15}). \text{MEK-PP}_L \\
\text{MEK-PP}_L &\stackrel{\text{def}}{=} (k8product, k_8). \text{MEK-PP}_H + (k7react, k_7). \text{MEK-PP}_H \\
&\quad + (k14product, k_{14}). \text{MEK-PP}_H \\
\text{ERK-PP}_H &\stackrel{\text{def}}{=} (k3react, k_3). \text{ERK-PP}_L \\
\text{ERK-PP}_L &\stackrel{\text{def}}{=} (k8product, k_8). \text{ERK-PP}_H + (k4react, k_4). \text{ERK-PP}_H \\
\text{ERK-P}_H &\stackrel{\text{def}}{=} (k6react, k_6). \text{ERK-P}_L \\
\text{ERK-P}_L &\stackrel{\text{def}}{=} (k5product, k_5). \text{ERK-P}_H + (k7react, k_7). \text{ERK-P}_H \\
\text{MEK-PP/ERK}_H &\stackrel{\text{def}}{=} (k8product, k_8). \text{MEK-PP/ERK}_L + (k7react, k_7). \text{MEK-PP/ERK}_L \\
\text{MEK-PP/ERK}_L &\stackrel{\text{def}}{=} (k6react, k_6). \text{MEK-PP/ERK}_H \\
\text{Raf-1}^*/\text{RKIP}_H &\stackrel{\text{def}}{=} (k3react, k_3). \text{Raf-1}^*/\text{RKIP}_L + (k2react, k_2). \text{Raf-1}^*/\text{RKIP}_L \\
\text{Raf-1}^*/\text{RKIP}_L &\stackrel{\text{def}}{=} (k1react, k_1). \text{Raf-1}^*/\text{RKIP}_H + (k4react, k_4). \text{Raf-1}^*/\text{RKIP}_H \\
\text{Raf-1}^*/\text{RKIP/ERK-PP}_H &\stackrel{\text{def}}{=} (k5product, k_5). \text{Raf-1}^*/\text{RKIP/ERK-PP}_L \\
&\quad + (k4react, k_4). \text{Raf-1}^*/\text{RKIP/ERK-PP}_L \\
\text{Raf-1}^*/\text{RKIP/ERK-PP}_L &\stackrel{\text{def}}{=} (k3react, k_3). \text{Raf-1}^*/\text{RKIP/ERK-PP}_H \\
\text{RKIP-P}_H &\stackrel{\text{def}}{=} (k9react, k_9). \text{RKIP-P}_L \\
\text{RKIP-P}_L &\stackrel{\text{def}}{=} (k5product, k_5). \text{RKIP-P}_H + (k10react, k_{10}). \text{RKIP-P}_H \\
\text{RP}_H &\stackrel{\text{def}}{=} (k9react, k_9). \text{RP}_L \\
\text{RP}_L &\stackrel{\text{def}}{=} (k11product, k_{11}). \text{RP}_H + (k10react, k_{10}). \text{RP}_H \\
\text{RKIP-P/RP}_H &\stackrel{\text{def}}{=} (k11product, k_{11}). \text{RKIP-P/RP}_L + (k10react, k_{10}). \text{RKIP-P/RP}_L \\
\text{RKIP-P/RP}_L &\stackrel{\text{def}}{=} (k9react, k_9). \text{RKIP-P/RP}_H
\end{aligned}$$

Fig. 2. PEPA model definitions for the reagent-centric model

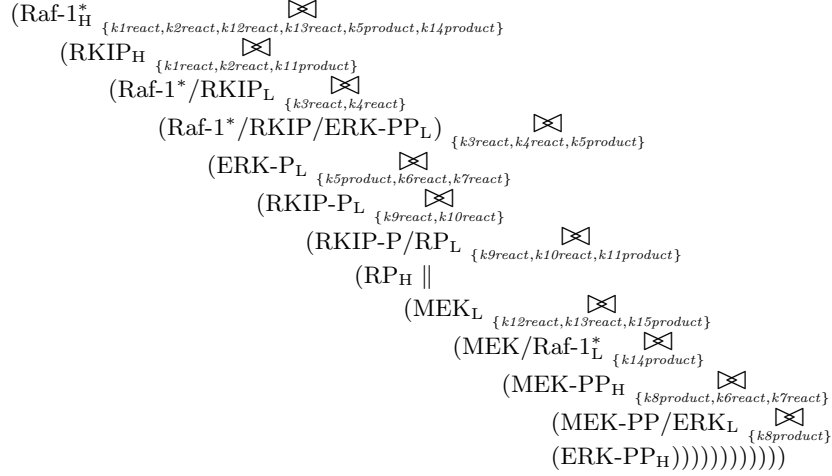


Fig. 3. PEPA model configuration for the reagent-centric model

4 Comparison of reagent and pathway-centric models

The pathway-centric model captures longer chains of behaviour flow within the system, leading to a smaller number of component definitions. Differentiating fewer components in the pathways model leads to a simpler composition of model components, presented in Figure 5. This is not only a matter of presentation. A larger state vector representation occupies more memory so the pathway-centric representation could potentially scale better to more detailed models of the Ras/Raf-1/MEK/ERK signalling pathway than the reagent-centric representation. But, the disadvantage of the pathway-centric representation is that it is no longer possible to read off directly concentrations of components (i.e. there is no explicit high or low concentrations). These now have to be inferred from local observations of pathways. This is relatively easy for proteins which have initial concentrations, otherwise, the inference is non-trivial.

Fortunately, the two models are observationally equivalent, that is, the two models give rise to (timing aware) bisimilar—in fact *isomorphic*—labelled multi-transition systems. We demonstrate this relationship by plotting the statespace of the two systems, see Figure 7. There are 28 states, s_1 to s_{28} , thus it is not possible in Figure 7 to give meaningful labels. In Table 2 we enumerate a few of the states. We give the name from the reagent-centric model first, followed by the name of the equivalent state from the pathway-centric model. In all cases, the synchronisation operator \bowtie is removed.

We believe that for any pathway, bisimilarity holds for any pair of reagent-centric and pathway-centric models; a formal proof is beyond the scope of this paper. We restrict our attention to this pathway and the consequence of the

$$\begin{aligned}
Pathway_{10} &\stackrel{def}{=} (k9react, k_9).Pathway_{11} \\
Pathway_{11} &\stackrel{def}{=} (k11product, k_{11}).Pathway_{10} + (k10react, k_{10}).Pathway_{10} \\
\\
Pathway_{20} &\stackrel{def}{=} (k1react, k_1).Pathway_{21} \\
Pathway_{21} &\stackrel{def}{=} (k3react, k_3).Pathway_{22} + (k2react, k_2).Pathway_{20} \\
Pathway_{22} &\stackrel{def}{=} (k5product, k_5).Pathway_{23} + (k4react, k_4).Pathway_{21} \\
Pathway_{23} &\stackrel{def}{=} (k9react, k_9).Pathway_{24} \\
Pathway_{24} &\stackrel{def}{=} (k11product, k_{11}).Pathway_{20} + (k10react, k_{10}).Pathway_{23} \\
\\
Pathway_{30} &\stackrel{def}{=} (k3react, k_3).Pathway_{31} \\
Pathway_{31} &\stackrel{def}{=} (k5product, k_5).Pathway_{32} + (k4react, k_4).Pathway_{30} \\
Pathway_{32} &\stackrel{def}{=} (k6react, k_6).Pathway_{33} \\
Pathway_{33} &\stackrel{def}{=} (k8product, k_8).Pathway_{30} + (k7react, k_7).Pathway_{32} \\
\\
Pathway_{40} &\stackrel{def}{=} (k1react, k_1).Pathway_{41} + (k12react, k_{12}).Pathway_{43} \\
Pathway_{41} &\stackrel{def}{=} (k2react, k_2).Pathway_{40} + (k3react, k_3).Pathway_{42} \\
Pathway_{42} &\stackrel{def}{=} (k5product, k_5).Pathway_{40} + (k4react, k_4).Pathway_{41} \\
Pathway_{43} &\stackrel{def}{=} (k13react, k_{13}).Pathway_{40} + (k14product, k_{14}).Pathway_{40} \\
\\
Pathway_{50} &\stackrel{def}{=} (k15product, k_{15}).Pathway_{51} + (k6react, k_6).Pathway_{53} \\
Pathway_{51} &\stackrel{def}{=} (k12react, k_{12}).Pathway_{52} \\
Pathway_{52} &\stackrel{def}{=} (k13react, k_{13}).Pathway_{51} + (k14product, k_{14}).Pathway_{50} \\
Pathway_{53} &\stackrel{def}{=} (k8product, k_8).Pathway_{50} + (k7react, k_7).Pathway_{50}
\end{aligned}$$

Fig. 4. PEPA model definitions for the pathway-centric model

$$\begin{aligned}
&(((Pathway_{50} \boxtimes_{\{k12react, k13react, k14product\}} Pathway_{40}) \\
&\quad \boxtimes_{\{k3react, k4react, k5product, k6react, k7react, k8product\}} Pathway_{30}) \\
&\quad \boxtimes_{\{k1react, k2react, k3react, k4react, k5product\}} Pathway_{20}) \\
&\quad \boxtimes_{\{k9react, k10react, k11product\}} Pathway_{10})
\end{aligned}$$

Fig. 5. PEPA model configuration for the pathway-centric model

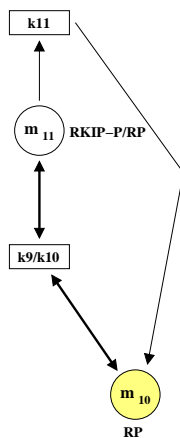


Fig. 6. *Pathway₁₀*

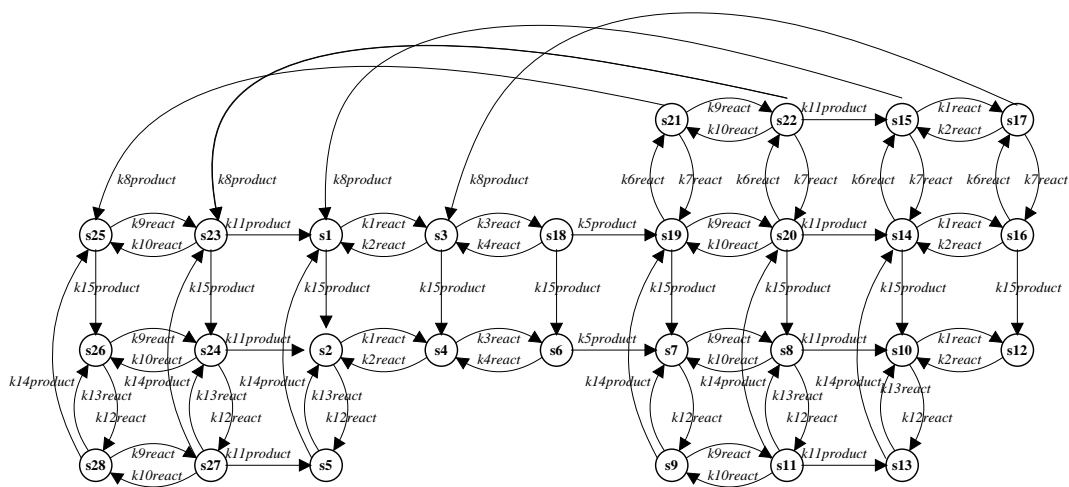


Fig. 7. The state space of the reagent and the pathway model

	Raf-1*	RKIP	Raf-1*/RKIP	Raf-1*/RKIP/ERK-PP	ERK-P	RKIP-P	RKIP-P/RP	RP	MEK	MEK/Raf-1*	MEK-PP	MEK-PP/ERK	ERK-PP	
s_1	(H, H, L, L, L, L, L, H, L, L, H, L, H)	(Pwy ₅₀ , Pwy ₄₀ , Pwy ₃₀ , Pwy ₂₀ , Pwy ₁₀)												
s_2	(H, H, L, L, L, L, L, H, H, L, L, L, H)	(Pwy ₅₁ , Pwy ₄₀ , Pwy ₃₀ , Pwy ₂₀ , Pwy ₁₀)												
s_3	(L, L, H, L, L, L, L, H, L, L, H, L, H)	(Pwy ₅₀ , Pwy ₄₁ , Pwy ₃₀ , Pwy ₂₁ , Pwy ₁₀)												
s_4	(L, L, H, L, L, L, L, H, H, L, L, L, H)	(Pwy ₅₁ , Pwy ₄₁ , Pwy ₃₀ , Pwy ₂₁ , Pwy ₁₀)												
s_5	(L, H, L, L, L, L, L, H, L, H, L, L, H)	(Pwy ₅₂ , Pwy ₄₃ , Pwy ₃₀ , Pwy ₂₀ , Pwy ₁₀)												
s_6	(L, L, L, H, L, L, L, H, H, L, L, L, L)	(Pwy ₅₁ , Pwy ₄₂ , Pwy ₃₁ , Pwy ₂₂ , Pwy ₁₀)												
s_7	(H, L, L, L, H, H, L, H, H, L, L, L, L)	(Pwy ₅₁ , Pwy ₄₀ , Pwy ₃₂ , Pwy ₂₃ , Pwy ₁₀)												
s_8	(H, L, L, L, H, L, H, L, H, L, L, L, L)	(Pwy ₅₁ , Pwy ₄₀ , Pwy ₃₂ , Pwy ₂₄ , Pwy ₁₁)												
s_9	(L, L, L, L, H, H, L, H, L, H, L, L, L)	(Pwy ₅₂ , Pwy ₄₃ , Pwy ₃₂ , Pwy ₂₃ , Pwy ₁₀)												
s_{10}	(H, H, L, L, H, L, L, H, H, L, L, L, L)	(Pwy ₅₁ , Pwy ₄₀ , Pwy ₃₂ , Pwy ₂₀ , Pwy ₁₀)												
\vdots	\vdots	\vdots												
s_{28}	(L, L, L, L, L, H, L, H, L, H, L, L, H)	(Pwy ₅₂ , Pwy ₄₃ , Pwy ₃₀ , Pwy ₂₃ , Pwy ₁₀)												

Table 2. Some bisimilar states

bisimilarity result which is that the two models give rise to the same Markov chain representations. The Markov chain can be analysed for *transient* behaviour, or solved to find the *steady-state* (long-run) probability distribution. Here we concentrate on the latter, since it is of more interest with respect to this pathway. In the following section we generate the steady state distribution and perform some analysis.

5 Model analysis

We used the PEPA Workbench [9] to analyse our models. The Workbench implements the operational semantics of PEPA to generate Continuous-Time Markov Chain (CTMC) models of system descriptions, and it provides analysis tools. First, we used the Workbench to test for deadlocks in our models. Initially, there were several; this is how we discovered an incompleteness in the system description of [5], with respect to with MEK. Second, when we had deadlock-free models, we used the Workbench to generate the CTMC and analyse its long-run probability distribution. This distribution varies as the rates associated with the activities of the PEPA model are varied, so the solution of the model is relative to a particular assignment of the rates.

The steady-state probability distribution can be obtained using a number of routines from numerical linear algebra. In the case of the present model(s), we solved this using the implementation of the preconditioned biconjugate gradient method in the PEPA Workbench. This is an iterative procedure which solves systems of linear equations of moderate size very quickly.

Numerical methods based on the computation of the steady-state probability distribution for a Continuous-Time Markov Chain have wide application, but are not routinely used in computational biology. Instead biological models are often formulated as systems of first-order coupled ordinary differential equations (ODEs) and computational analysis proceeds via reaction rate equations using methods such as Runge-Kutta.

In another paper [3], we present an algorithmic procedure for generating a system of ODEs from a PEPA model of high and low component concentration. This provides a useful method of validating a process algebra model against an existing system of ODEs. In the case of the ERK pathway we have been able to recreate exactly the system of ODEs as used in [5].

Numerical integration of the ODEs gives rise to time series plots which show how the concentration of components varies over time. These tend to a steady-state equilibrium which we have found to be in good agreement with the steady-state computed by Markovian methods.

Because of this different point of view it is appropriate to say a little here about how computational analysis via CTMCs compares with analysis via ODEs.

There are two axes of comparison for numerical methods. One is numerical stability (that is, under what conditions the methods converge to an acceptable result) and the other is computational efficiency. To make both parts of the comparison between CTMCs and ODEs we consider using the Chapman-Kolmogorov differential equations to perform transient analysis of a Markov chain.

Firstly, in the seminal work on numerical solution of Markov chains Stewart [19] discourages the use of ODEs to perform transient analysis of Markov chains, pointing to poor stability properties. Thus Markovian methods have this advantage in practical application.

Secondly, although it is more informative, transient analysis has higher computational cost than steady-state analysis. This indicates a saving in computational cost because here we are considering only steady-state solutions of the reagent and pathway models.

Since the reagent and pathway models are isomorphic, the underlying steady-state probability distributions are identical. However, it is possible to make different judgements about the two models using the PEPA state-finder which allows one to search for symbolic descriptions of states. For example, in the reagent-centric model, we used the PEPA state-finder to aggregate the probabilities of all states when ERK-PP is high, or low, for a given set of rates. That is, it aggregated the probabilities of states whose (symbolic) description has the form $* \bowtie \text{ERK-PP}_H$ where $*$ is a wildcard standing for any expression. We then repeated this with a different set of rates and compared results. In the reagent-centric model, we observed that the probability of being in a state with

ERK-PP_H *decreases* as the rate $k1$ is increased, and the converse for ERK-PP_L *increases*. For example, with $k1 = 1$ and $k1 = 100$, the probability of ERK-PP_H drops from .257 to .005. We can also plot throughput (rate \times probability) against rate. Figures 8 and 9 shows two sub-plots which detail the effect of increasing the rate $k1$ on the $k14product$ and $k8product$ reactions – the production of (doubly) phosphorylated MEK and (doubly) phosphorylated ERK, respectively. These are obtained by solving the pathway model, taking each of the product and reaction rates to be unity and scaling $k1$ (keeping all other rates to be unity). The graphs show that increasing the rate of the binding of RKIP to Raf-1* dampens down the $k14product$ and $k8product$ reactions, and they quantify this information. The efficiency of the reduction is greater in the former case: the graph falls away more steeply. In the latter case the reduction is more gradual and the throughput of $k8product$ peaks at $k1 = 1$. Note that since $k5product$ is on the same pathway as $k8product$, both ERK-PP and ERK-P are similarly affected. Thus we conclude that the rate at which RKIP binds to Raf-1* (thus suppressing phosphorylation of MEK) affects the ERK pathway, as predicted (and observed); RKIP does indeed regulate the ERK pathway.

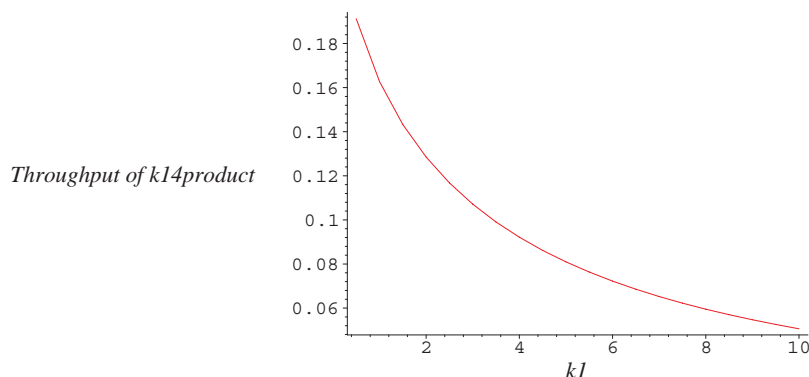


Fig. 8. Plotting the effect of $k1$ on $k14product$

6 Transformation

In this section we present a set of transformations between the two styles of representation, based on an intermediate matrix representation. Thus we define an *activity matrix* M_a which captures the relationship between reagents and reactions. The matrix has one row corresponding to each reagent in the system, whilst each column corresponds to exactly one reaction. Within the matrix we quantify the impact of each reaction on each reagent in a manner analogous to

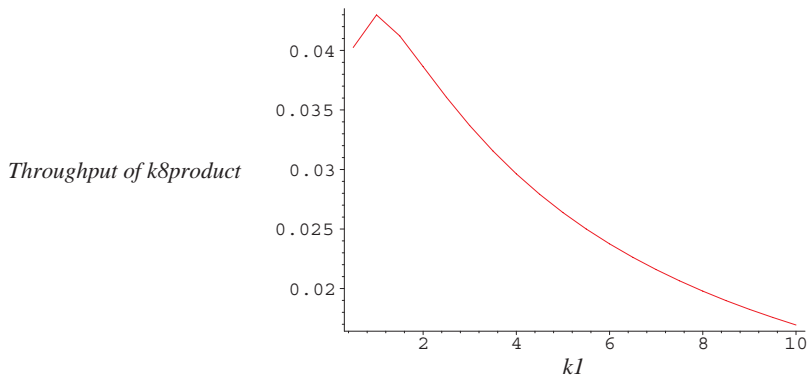


Fig. 9. Plotting the effect of $k1$ on $k8product$

the stoichiometry matrix of the chemical reaction³. This can be regarded as a canonical representation in the sense that there is no redundancy within it. In the example presented in this paper all reactions are deterministic and therefore entries in the activity matrix will always be between -1 , 0 or $+1$.

As we will show, both reagent-centric and pathway-centric PEPA models can be readily and systematically translated into their activity matrix representation. Moreover, we will also show that for a given activity matrix a corresponding PEPA model of either form can be systematically generated. In the remainder of this section we give the algorithms for each of these transformations — from the process algebra models to the matrix, and from the matrix to each form of process algebra model.

Definition 1 (Activity Matrix). *For a system with R reactions and S reagents, the activity matrix M_a is an $S \times R$ matrix, and the entries are defined as follows.*

$$(s_i, r_j) = \begin{cases} +1 & \text{if } s_i \text{ is a consumer of } r_j \\ -1 & \text{if } s_i \text{ is a producer of } r_j \\ 0 & \text{otherwise.} \end{cases}$$

The relationship between the activity matrix the reagent-centric model is fairly straightforward but the relationship to the pathway model is somewhat more involved. Therefore we start by explaining the mapping from the reagent-centric model to the matrix.

Reagent-centric model to activity matrix In the reagent centric model there are a pair of PEPA definitions corresponding to each reagent. The set of reactions that this reagent is involved in are those that appear in the definitions of these components. The impact of a reaction can be seen according to whether the reaction

³ However, we emphasise that our models do not represent individual molecules

moves the reagent from high to low (decreasing, -1) or vice versa (increasing, $+1$). The algorithm for generating the activity matrix from a reagent-centric model is shown in Figure 10.

```
// Construct a matrix of the appropriate size
Form a matrix with one row for each pair (H,L) of components
and a column for each activity used in the process algebra definitions

// Populate the matrix
For each H component, on the appropriate row, make a -1 entry in the
column corresponding to each activity it enables
For each L component, on the appropriate row, make a +1 entry in the
column corresponding to each activity it enables
```

Fig. 10. Pseudo-code for transforming a reagent-centric model to an activity matrix

Activity matrix to reagent-centric model When forming a reagent-centric PEPA model from an activity matrix, we will generate two PEPA component definitions for each reagent/row of the matrix – one corresponding to high concentration and one corresponding to low concentrations. The reagent in high concentration will enable all those reactions which have a negative entry in the column, whilst the reagent in low concentration will enable all those reactions which have a positive entry in the column.

The algorithm for generating a reagent-centric model from an activity matrix is shown in Figure 11. There are two stages to the algorithm. First, a pair of model components are formed corresponding to each row as outlined above. Second, the components must be configured with appropriate interactions between them. We exploit the knowledge that in this style of model each component must cooperate on all its activities. Thus the model configuration is built iteratively — as each component is added it is specified to cooperate with *the rest of the model* on all its activities. Whether each reagent exhibits its high or low concentration form in the configuration depends on whether experimental data suggests it starts with initial concentration or not.

Pathway-centric model to activity matrix The algorithm for generating the activity matrix from a pathway-centric model is shown in Figure 12. The construction of the matrix to capture the involvement of pathway model components in the reactions of the system is straightforward. However, this construction will result in some duplicate rows within the matrix because some compound reagents can be seen to be intermediate states of two or more pathways (e.g. RKIP-P/RP corresponds to both Pwy_{11} and Pwy_{12}). Thus the duplicates must be removed.

Activity matrix to pathway-centric model The algorithm for generating a pathway-centric model from an activity matrix is shown in Figure 13. In the activity

```

// Form the model components
For each row of the matrix assign a reactant name.
For each reactant
  make a H subscripted component based on the reactant name
  define this component to be a choice of activities as follows:
    for each -1 in the corresponding row of the activity matrix
      make an activity of the type of the appropriate column
      which results in an L subscripted component of the same name
      add this activity to the choice for the H component
  make an L subscripted component based on the reactant name
  define this component to be a choice of activities as follows:
    for each +1 in the corresponding row of the activity matrix
      make an activity of the type of the appropriate column
      which results in an H subscripted component of the same name
      add this activity to the choice for the L component

// Form the model configuration
For each reactant
  if this reagent has high initial concentration
    enter the H subscripted component
  if this reagent has low initial concentration
    enter the L subscripted component
  // build the appropriate cooperation set K
  for each non-zero entry of the corresponding row of the activity matrix
    enter the corresponding reaction/activity to the set K
  add a cooperation over the set K and "("
add one ")" for each row of the matrix

```

Fig. 11. Pseudo-code for transforming an activity matrix to a reagent-centric model

```

// Construct a matrix of the appropriate size
Form a matrix with one row for each of the components exhibited by the pathways
and a column for each activity used in the process algebra definitions

// Populate the matrix
For each component, on the appropriate row, make a -1 entry in the
column corresponding to each activity it enables and a +1 entry in
the same column of the resulting component.

//Reduce the matrix
Detect and remove identical rows

```

Fig. 12. Pseudo-code for transforming a pathway-centric model to an activity matrix

matrix each row corresponds to a distinct reagent. In order to reconstruct the sub-pathways, we need to take into account that fact that some reagents may correspond to intermediate states in two or more pathways. Thus we introduce a notion of colouring, in which one colour is associated with each sub-pathway. A single row/reagent may have several colourings indicating which sub-pathways it participates in.

The next goal is to identify the sub-pathways. We note that for all reagents all the reactions that they participate in will be part of the same sub-pathway although it is not true that each reagent that participates in a reaction will belong to the same sub-pathway. Consequently either all the entries in a row will be coloured with some colour C or none will. However, except for the rows corresponding to initial concentrations, which are taken as the roots of our sub-pathways, any row may have any number of colours associated with it.

In order to find the sub-pathways we need to find a consumer corresponding to each producer, and vice versa, within each colour. Once such an association is made we consider the coloured matrix entry to be *paired*. The pathway is complete when all entries of that colour have been paired. In some cases there may be several candidate matrix entries for forming a pair: the corresponding rows are collected into a set of provisionally coloured rows until it becomes clear which entry completes a minimal cycle. The other rows are then discarded.

When, for each colour, all matrix entries are paired, the sub-pathway model components can be defined in a straightforward way. It remains to form the model component. Those entries which have more than one colour must be carried out in cooperation by the corresponding pathways. Thus, for a pathway component with colour C , the cooperation set is formed as those reactions corresponding to a column in the matrix in which there is an entry which is coloured C and some other colour.

As an illustration we present the activity matrix corresponding to the example presented earlier in the paper in Figure 14. This can be derived from either the reagent- or the pathway-centric model. In the far right hand column we give an indication of the colouring of the matrix to derive the pathway model shown in Figure 4 — the numbers indicate which pathway(s) each row corresponds to.

7 Further Analysis

The process algebraic approach has several tangible benefits. For example, in addition to deadlock and quantitative analysis, the compositional nature of the process algebra approach confines changes to the behaviour of a reagent to a single system component, i.e. to one or two equations. In an ODE model, such a change would be pervasive, i.e. numerous equations would have to be altered. Nevertheless, ODE models offer analysis by a wide variety of solvers. In [3] we show how an ODE model defining standard mass action kinetics can be derived automatically from the process algebra reagent-centric or pathway-centric models, via the activity matrix. A key observation is that the coarsest level of abstraction (i.e. *high* and *low*) provides sufficient information for deriving the ODE

```

// Colour assignment
Assign a unique colour to each reagent which has initial concentration
Identify the rows of the matrix corresponding to these reagents
Colour each row accordingly

// Find minimal pathways
For each colour C
    while there are unpaired C entries in the matrix
        for each -1(resp. +1) entry in row s and column r coloured C
            find all entries in column r
                if there are more than one +1(resp. -1) entry
                    if none are already coloured C
                        provisionally colour each corresponding entry
                        record them as a row set
                if there is only one +1(resp. -1) entry, in row s' say
                    if it is not already coloured C
                        colour row s' with colour C
                    if s' was previously provisionally coloured with C
                        remove the provisional colouring from all other
                        elements of the row set

// Form the model components
For each colour C
    make an initial Pathway component
    make a Pathway component for each other row with C coloured entries
    for each C coloured Pathway component/row
        define the pathway component with one activity corresponding
        to each -1 column in the row whose resulting component will
        be the C coloured +1 entry in the same column

// Form the model configuration
For each colour C
    enter the corresponding initial Pathway component
    for each reaction r which is coloured C and another colour C'
        enter r into the cooperation set K
    add a cooperation over the set K and "("
add one ")" for each colour

```

Fig. 13. Pseudo-code for transforming an activity matrix to a pathway-centric model

	$k1$	$k2$	$k3$	$k4$	$k5$	$k6$	$k7$	$k8$	$k9$	$k10$	$k11$	$k12$	$k13$	$k14$	$k15$	pathways
Raf-1*	-1	+1	0	0	+1	0	0	0	0	0	0	-1	+1	+1	0	4
RKIP	-1	+1	0	0	0	0	0	0	0	0	+1	0	0	0	0	2
Raf-1*/RKIP	+1	-1	-1	+1	0	0	0	0	0	0	0	0	0	0	0	2, 4
Raf-1*/RKIP/ERK-PP	0	0	+1	-1	-1	0	0	0	0	0	0	0	0	0	0	2, 3, 4
ERK-P	0	0	0	0	+1	-1	+1	0	0	0	0	0	0	0	0	3
RKIP-P	0	0	0	0	+1	0	0	0	-1	+1	0	0	0	0	0	2
MEK-PP	0	0	0	0	0	-1	+1	+1	0	0	0	0	0	+1	-1	5
MEK-PP/ERK	0	0	0	0	0	+1	-1	-1	0	0	0	0	0	0	0	3, 5
ERK-PP	0	0	-1	+1	0	0	0	+1	0	0	0	0	0	0	0	3
RP	0	0	0	0	0	0	0	0	-1	+1	+1	0	0	0	0	1
RKIP-P/RP	0	0	0	0	0	0	0	0	+1	-1	-1	0	0	0	0	1, 2
MEK	0	0	0	0	0	0	0	0	0	0	0	-1	+1	0	+1	5
MEK/Raf-1*	0	0	0	0	0	0	0	0	0	0	0	+1	-1	-1	0	4, 5

Fig. 14. Activity matrix of the ERK pathway

representation. In other words, it is sufficient to know which reactions increase concentration (i.e. low to high), and which ones decrease concentration (i.e. high to low). The addition of further discrete values does not add further information. Thus all the standard analysis tools available for ODEs are also available to the modeller taking the process algebraic approach with the coarsest (and simplest) discretisation of concentrations.

Further quantitative analysis is possible using probabilistic logics and probabilistic model checking. For example, we have investigated the use of the logic CSL [1] and the model checker PRISM [12]. Further analysis of a PRISM model derived from the reagent-centric model given here is reported in [4]. Examples of CSL properties (stated informally) are “*What is the probability that a concentration of a species reaches a particular value and then remains at that value thereafter?*”, and “*How does varying a reaction rate affect that probability?*”. We note that in this paradigm, the resulting probabilities depend on the granularity of discrete concentration values.

8 Related Work

The work of Regev and her co-authors has been deeply influential [16, 18, 15, 17]. Although the exact form of the process algebra which is used in these works varies, there is some commonality in the languages and the analysis is always based on stochastic simulation. At the basis is always the fundamental mapping developed by Regev in her thesis. In this mapping a correspondence is made

between molecules in the biological system and processes or agents in the process algebra.

In this paper we propose a different mapping in which a correspondence is made between a subpathway and a process in the process algebra. The most basic form of subpathway is taken to be a single species and its fluctuations in concentrations. In the paper we have demonstrated this and a larger notion of subpathway based on the notion of the possible biochemical flow of a single species. The key point is that this mapping is onto an abstract concept in the biology (the species or pathway) rather than a concrete one (the molecule). We believe that this shift to the more abstract form offers an alternative view of systems and better access to the analysis mechanisms associated with process algebras.

The work of Fisher *et al.* reported in [8] also proposes using two distinct views of the same system. However, they envisage different roles for the two views, one capturing the observations of a system which have been made experimentally (scenario-based model) and the other making an hypothesis about the mechanistic behaviour which might generate such observations (state-based model). In their terminology, both our models are state-based, seeking to give a mechanistic account for how observed behaviour may arise. It is an interesting area for future work to consider how this might be formally reconciled with experimental observations.

The pathway view of our network bears some resemblance to the *extreme pathways* (and the related concept of *elementary modes*) in the work of Papin *et al.* on metabolic pathways [14]. There the authors aim to identify and separate subpathways using linear algebra techniques applied to the stoichiometry matrix for a metabolic pathway. The exact relationship with our own work is an area for further work.

In theoretical computer science it has previously been remarked that process algebra models may be used to capture the same system in a variety of different styles e.g. [20]. We view our work as continuing in that tradition, for example our modelling styles loosely correspond to the constraint oriented style, although in a different context and considering somewhat different styles of model. As we continue to explore the relationship between our modelling styles we hope to be able to benefit from this earlier research.

9 Conclusions

We have presented two alternative PEPA models of the Raf-1/MEK/ERK module of the ERK signalling pathway and shown them to be equivalent. The reagent-based model has explicit concentrations whilst in the pathway model the concentrations are captured only implicitly via the possible activities of each sub-pathway. The pathway-based model can thus be regarded as less directly expressive, although it captures all the same behaviour. The congruence results of PEPA with respect to strong bisimulation mean that the two representations may be used interchangeably, for example within a large model. Thus we might

envisage a model in which the key pathway is modelled using the reagent-style whilst peripheral pathways are modelled using the pathway-style. Or, we may have one style of model and hypothesise the other. We believe this ability to have different views is novel in the field of modelling pathways; informal discussions with biologists confirm their interest in it.

We found the multi-way synchronisation of PEPA, and the performance aspects, to be ideally suited to modelling pathway behaviour. In this example, deadlock analysis very quickly revealed an incompleteness in the published model. Once deadlock-free, one strength of models of the kind which we have used here is that they give rise to compact Markov chain representations which can be efficiently solved for different assignments to the rate variables in a series of experiments. This delivers the benefit that a thorough series of experiments can be conducted at modest computational cost.

Furthermore, we have presented transformations between the two alternative styles of representation, via an intermediate, the *activity matrix*. This means that automatic translation between representations is possible. The transformation from an activity matrix to the pathway model has some similarities with finding the minimal T-semiflows of a Petri net. Comparing our algorithm with the algorithms for T-semiflows [6], or the more general mathematical programming problem of finding the extremal directions of a cone [13], are yet to be investigated.

Process algebra opens up a host of analysis possibilities, including, in addition to Markov chain analysis, the use of ODE solvers and reasoning with probabilistic logics using probabilistic model checking. With respect to the former, we have found we require only to distinguish between high and low concentrations, further granularity adds no analytic benefit. Rather we need only model the *direction* of change (i.e. an increase or decrease of concentration). With respect to the latter, we have conducted initial investigations with the logic CSL and indicated further possibilities.

Several challenges remain. For example, we wish to derive the reagent-centric model from experimental data and model spatial aspects of pathways. We have some preliminary ideas which are the topic of future research.

Acknowledgements

Stephen Gilmore and Jane Hillston are supported by the SENSORIA (Software Engineering for Service-Oriented Overlay Computers) 6th framework Global Computing Initiative IST project funded by the European Union. Jane Hillston is funded by an Advanced Research Fellowship from the UK Engineering and Physical Sciences Research Council. Muffy Calder is supported by the DTI Beacon Bioscience Projects programme and thanks Walter Kolch, Beatson Cancer Research Centre, and Rainer Breitling, David Gilbert, Richard Orton, and Oliver Sturm from the Bioinformatics Research Centre, University of Glasgow, for helpful discussions.

References

1. A. Aziz, K. Sanwal, V. Singhal, and R. Brayton. Verifying continuous time Markov chains. In *Computer-Aided Verification*, volume 1102 of *LNCS*, pages 169–276. Springer-Verlag, 1996.
2. M. Calder, S. Gilmore, and J. Hillston. Modelling the influence of RKIP on the ERK signalling pathway using the stochastic process algebra PEPA. In *Proc. of BioConcur 2004*, pages 26–41. Danmarks Tekniske Universitet, 2004. To appear in ENTCS.
3. M. Calder, S. Gilmore, and J. Hillston. Automatically deriving ODEs from process algebra models of signalling pathways. In *Computational Methods in Systems Biology 2005*, pages 204–215. LFCS, University of Edinburgh, 2005.
4. M. Calder, V. Vyshemirsky, R. Orton, and D. Gilbert. Analysis of signalling pathways using the PRISM model checker. In *Computational Methods in Systems Biology 2005*, pages 179–190. LFCS, University of Edinburgh, 2005.
5. K.-H. Cho, S.-Y. Shin, H.-W. Kim, O. Wolkenhauer, B. McFerran, and W. Kolch. Mathematical modeling of the influence of RKIP on the ERK signaling pathway. In C. Priami, editor, *Computational Methods in Systems Biology (CSMB'03)*, volume 2602 of *LNCS*, pages 127–141. Springer-Verlag, 2003.
6. J.M. Colom and M. Silva. Convex geometry and semiflows in P/T nets. a comparative study of algorithms for computation of minimal P-semiflows. In G. Rozenberg, editor, *Advances in Petri Nets 1990*, volume 483 of *LNCS*, pages 79–112. Springer-Verlag, 1991.
7. W.H. Elliot and D.C. Elliot. *Biochemistry and Molecular Biology, 2nd edition*. Oxford University Press, 2002.
8. J. Fisher, D. Harel, E.J.A. Hubbard, N. Piterman, M.J. Stern, and N. Swerdlin. Combining state-based and scenario-based approaches in modeling biological systems. In V. Danos and V. Schachter, editors, *Computational Methods in Systems Biology 2004*, volume 3082 of *LNBI*, pages 236–241. Springer, 2005.
9. S. Gilmore and J. Hillston. The PEPA Workbench: A Tool to Support a Process Algebra-based Approach to Performance Modelling. In *Proceedings of the Seventh International Conference on Modelling Techniques and Tools for Computer Performance Evaluation*, number 794 in *Lecture Notes in Computer Science*, pages 353–368, Vienna, May 1994. Springer-Verlag.
10. M. Heiner and I. Koch. Petri net based model validation in systems biology. In *25th International Conference on Application and Theory of Petri Nets, Bologna, Italy*, 2004.
11. J. Hillston. *A Compositional Approach to Performance Modelling*. Cambridge University Press, 1996.
12. M. Kwiatkowska, G. Norman, and D. Parker. Probabilistic symbolic model checking with PRISM: A hybrid approach. In J.-P. Katoen and P. Stevens, editors, *Proc. 8th International Conference on Tools and Algorithms for the Construction and Analysis of Systems (TACAS'02)*, volume 2280 of *LNCS*, pages 52–66. Springer, April 2002.
13. T.H. Matheiss and D.S. Rubin. A survey and comparison of methods for finding all the vertices of convex polyhedral sets. *Mathematics of Operational Research*, 5(2):167–185, 1980.
14. J.A. Papin, N.D. Price, S.J. Wiback, D.A. Fell, and B.O. Palsson. Metabolic pathways in the post-genome era. *TRENDS in Biochemical Sciences*, 28(5):250–258, May 2003.

15. C. Priami, A. Regev, W. Silverman, and E. Shapiro. Application of a stochastic name passing calculus to representation and simulation of molecular processes. *Information Processing Letters*, 80:25–31, 2001.
16. A. Regev. *Computational Systems Biology: a Calculus for Biomolecular Knowledge*. PhD thesis, Tel Aviv University, 2002.
17. A. Regev, E.M. Panina, W. Silverman, L. Cardelli, and E. Shapiro. BioAmbients: an abstraction for biological compartments. *Theoretical Computer Science*, 325(1):141–167, 2004.
18. A. Regev, W. Silverman, and E. Shapiro. Representation and simulation of biochemical processes using the pi-calculus process algebra. In *Proceedings of the Pacific Symposium of Biocomputing (PSB2001)*, pages 459–470, 2001.
19. William Stewart. *Numerical Solution of Markov Chains*. Princeton University Press, 1994.
20. C.A. Vissers, G. Scollo, M. van Sinderen, and E. Brinksma. Specification styles in distributed systems design and verification. *Theoretical Computer Science*, 89:179–206, 1991.

A PEPA

This appendix provides a brief introduction to PEPA in order to make the paper self-contained. It can safely be skipped by anyone who already knows the PEPA language. For a full explanation which complements the brief description presented here the reader is referred to [11].

Prefix: The basic mechanism for describing the behaviour of a system with a PEPA model is to give a component a designated first action using the prefix combinator, denoted by a full stop. For example, $(\alpha, r).S$ carries out activity (α, r) , which has action type α and an exponentially distributed duration with parameter r , and it subsequently behaves as S .

Choice: The component $P + Q$ represents a system which may behave either as P or as Q . The activities of both P and Q are enabled. The first activity to complete distinguishes one of them: the other is discarded. The system will behave as the derivative resulting from the evolution of the chosen component.

Constant: It is convenient to be able to assign names to patterns of behaviour associated with components. Constants are components whose meaning is given by a defining equation. The notation for this is $X \stackrel{\text{def}}{=} E$. The name X is in scope in the expression on the right hand side meaning that, for example, $X \stackrel{\text{def}}{=} (\alpha, r).X$ performs α at rate r forever.

Hiding: The possibility to abstract away some aspects of a component's behaviour is provided by the hiding operator, denoted P/L . Here, the set L identifies those activities which are to be considered internal or private to the component and which will appear as the unknown type τ .

Cooperation: We write $P \bowtie_L Q$ to denote cooperation between P and Q over L . The set which is used as the subscript to the cooperation symbol, the *cooperation set* L , determines those activities on which the *cooperands* are forced to synchronise. For action types not in L , the components proceed independently and concurrently with their enabled activities. We write $P \parallel Q$ as an abbreviation for $P \bowtie_L Q$ when L is empty.

However, if a component enables an activity whose action type is in the cooperation set it will not be able to proceed with that activity until the other component also enables an activity of that type. The two components then proceed together to complete the *shared activity*. The rate of the shared activity may be altered to reflect the work carried out by both components to complete the activity (for details see [11]).

In some cases, when an activity is known to be carried out in cooperation with another component, a component may be *passive* with respect to that activity. This means that the rate of the activity is left unspecified (denoted \top) and is determined upon cooperation, by the rate of the activity in the other component. All passive actions must be synchronised in the final model.